Optical Materials 46 (2015) 216–222

Contents lists available at ScienceDirect

Optical Materials

journal homepage: www.elsevier.com/locate/optmat

Theoretical investigation of some specific features of the electronic structure and optical properties of Benzoic Acid 2-Amino-4, 6-Dimethylpyrimidine (1:1) co-crystals

A.H. Reshak *

New Technologies – Research Centre, University of West Bohemia, Univerzitni 8, 306 14 Pilsen, Czech Republic
Center of Excellence Geopolymer and Green Technology, School of Material Engineering, University Malaysia Perlis, 01007 Kangar, Perlis, Malaysia

ARTICLE INFO

Article history:
Received 7 February 2015
Received in revised form 28 March 2015
Accepted 14 April 2015
Available online 30 April 2015

Keywords:
A. Electronic materials
Optical materials
C. Computer modeling and simulation
D. Crystal structure

ABSTRACT

Benzoic Acid 2-Amino-4,6-Dimethylpyrimidine (1:1) co-crystal have been comprehensively investigated by means of density functional theory. The electronic band structure show that the conduction band minimum (*CBM*) and the valence band maximum (*VBM*) are situated at the center of the Brillouin zone resulting in a direct band gap. Calculation were performed using the full potential linear augmented plane wave plus local orbitals ($FPLAPW + lo$) method in a scalar relativistic version as embodied in the *WIEN2k* code within the local density approximation (*LDA*), gradient approximation (*PBE-GGA*), Engel–Vosko generalized gradient approximation (*EV-GGA*) and the recently modified Becke–Johnson potential (*mBJ*). The calculated density of states explore that the *VBM* is mainly formed by N-p state while the *CBM* is formed by the strongly hybridized N-p and C-p states. There exists a strong hybridizations between C-s/p, H-s, N-s/p and O-s/p states above and below the Fermi level (E_F). Which may led to covalent bonding between the states. To visualizes the charge transfer and the chemical bonding characters, the valence band's electronic charge density distribution were extensively investigated. The optical properties helps to get deep insight into the electronic structure therefore, details analysis to the calculated optical properties were performed. The optical properties confirm the existence of the band gap and the lossless regions.

1. Introduction

Several experimental and theoretical research work on co-crystals is achieved due to their specific structure. It is found that the co-crystals are promising candidates for many applications due to their novel chemical and physical properties [1]. Benzoic Acid 2-Amino-4,6-Dimethylpyrimidine (1:1) is one of the co-crystals, in which the hydrogen bond interactions play an important role in composing the structure, etc. [2,3]. Therefore, it is necessary to investigate the hydrogen-bonded networks which are linked with mobile protons. From the hydrogen-bonded networks of the Benzoic Acid 2-Amino-4,6-Dimethylpyrimidine one can deduce very important information since the hydrogen-bonded networks are essential elements for the supermolecules in the biology systems and chemistry. Latajka et al. [4] theoretically investigated the hydrogen-bonded molecular complexes, they investigated the polarizability and first hyperpolarizability values of the hydrogen-bonded complexes formed by nitrosubstituted phenols with pyridine and 4-aminopyridine have been calculated using PM3 and *ab initio* (STO-3G) methods. Li et al. [1] have prepared the Benzoic Acid 2-Amino-4,6-Dimethylpyrimidine and analysis the single crystal X-ray diffraction data and the experimental optical properties. In addition they perform a density functional calculations using CASTEP code within generalized gradient approximation (*PBE-GGA*).

Due to a lack of electronic structural information of Benzoic Acid 2-Amino-4,6-Dimethylpyrimidine (1:1) co-crystal, further insight into the electronic structure can be obtained from the optical properties. We would like to mention that we are not aware of calculations or experimental data for the electronic structure and linear optical susceptibilities of Benzoic Acid 2-Amino-4,6-Dimethylpyrimidine (1:1) co-crystal. Therefore we thought it worthwhile to calculate some specific features of the electronic structure and the optical properties. Calculations are performed using full potential method within four types of exchange correlation potentials in order to ascertain the effect of exchange correlation on the electronic structure and the optical

* Tel.: +420 777729583; fax: +420 386 361255.
E-mail address: maalidph@yahoo.co.uk

http://dx.doi.org/10.1016/j.optmat.2015.04.022
0925-3467/

properties. First-principles calculation is one strong and useful tool to predict the crystal structure and its properties related to the electron configuration of a material before its synthesis [5–8].

2. Details of calculations

Benzoic Acid 2-Amino-4,6-Dimethylpyrimidine (1:1) co-crystal ($C_{13}H_{15}N_3O_2$) have been synthesized by Li et al. [1] from benzoic acid and 4,6-Dimethylpyrimidine in 1:1 molar ratio (see Fig. 1a). $C_{13}H_{15}N_3O_2$ crystallizes in a monoclinic structure, space group, $P2_1/c$ with lattice constants $a = 6.7019(9)$ Å, $b = 7.647(1)$ Å and $c = 25.285(3)$ Å, $\beta = 91.36(2)^\circ$, $V = 1295.4(3)$ Å^3, $Z = 4$ [1]. The 2-Amino-4,6-Dimethylpyrimidine molecule linked to benzoic acid molecule by two hydrogen bonds [$O1-H1\cdots N1, H\cdots N = 1.819$ Å; $N3-H3A\cdots O2, H\cdots O = 2.157$ Å] to form the asymmetric unit as shown in Fig. 1(a). Fig. 1(b) shows the discreet dimers are connected together in 1D-zigzag pattern. The calculation were performed using the density functional theory (*DFT*) within the full potential linear augmented plane wave plus local orbitals (*FPLAPW* + *lo*) method in a scalar relativistic version as embodied in the *WIEN2k* code [9]. The exchange-correlation (*XC*) potential was solved using four different possible approximations. The *XC* were described by the local density approximation (*LDA*) [10] and gradient approximation (*PBE-GGA*) [11], which is based on exchange-correlation energy optimization to calculate the total energy. In addition, we have used Engel–Vosko generalized gradient approximation (*EV-GGA*) [12] and the recently modified Becke–Johnson potential (*mBJ*) [13] which optimizes the corresponding potential for electronic band structure calculations. The atomic positions were optimized by minimization of the forces acting on each atom. The optimization were achieved within *PBE-GGA*. The structure is fully relaxed until the forces on the atoms reach values less than (1 mRy/a.u.). The optimized atomic positions along with those obtained from *XRD* are listed in Table S1 (supplementary materials), good agreement was found. Once the forces are minimized in this construction one can then find the self-consistent density at these positions by turning off the relaxations and driving the system to self-consistency. From the obtained relaxed geometry the electronic structure and the chemical bonding have been determined and various spectroscopic features can be simulated and compared with experimental data. The Kohn–Sham equations are solved using a basis of linear *APW′s*. The potential and charge density in the muffin-tin (*MT*) spheres are expanded in spherical harmonics with $l_{max} = 8$ and nonspherical components up to $l_{max} = 6$. In the interstitial region the potential and the charge density are represented by Fourier series. Self-consistency is obtained using 300 $\vec{k}$ points in the irreducible Brillouin zone (*IBZ*). We have calculated the electronic band structure, density of states, electronic charge density distribution and linear optical properties using 500 $\vec{k}$ points in the *IBZ*. The self-consistent calculations are converged since the total energy of the system is stable within 0.00001 Ry.

3. Results and discussion

3.1. Electronic band structure and density of states

The electronic band structure of Benzoic Acid 2-Amino-4,6-Dimethylpyrimidine is plotted along the high symmetry points $\Gamma, Y, H, X, A, Z, \Gamma, X$ in the first Brillouin zone (Fig. 2). To investigate the influence of the exchange-correlation potential on the electronic band desperation, four types of exchange-correlation potentials are used to calculate the electronic band structure. In all cases the Fermi level is sited to be at 0.0 eV. It is clear that moving from *LDA* to *PBE-GGA* to *EV-GGA* cause to shift the conduction band minimum (CBM) toward the higher energies by around 0.1 eV. Whereas using mBJ cause to shift the CBM toward higher energies by around 1.0 eV with respect to the location of CBM obtained by *LDA*. Calculation show that the valence band maximum (VBM) and CBM are situated at center of the *BZ*. Therefore, the Benzoic

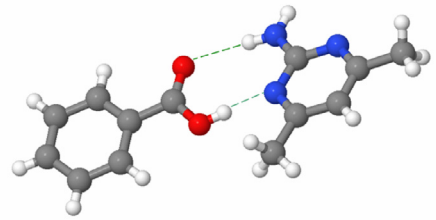

The 2-Amino-4,6-Dimethylpyrimidine molecule linked to benzoic acid molecule by two hydrogen bonds [$O1-H1...N1$, $H...N$ =1.815 Å; $N3-H3A...O2$, $H...O$ =2.149 Å] to form the asymmetric unit.

(a) Asymmetric unit

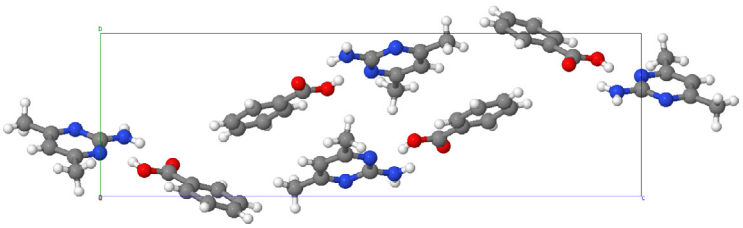

(b)

Fig. 1. (a) the asymmetric unit, it shows the 2-Amino-4,6-Dimethylpyrimidine molecule linked to benzoic acid molecule by two hydrogen bonds [$O1-H1\cdots N1, H\cdots N = 1.815$ Å; $N3-H3A\cdots O2, H\cdots O = 2.149$ Å] to form the asymmetric unit. (b) Fragment of the crystal structure of Benzoic Acid 2-Amino-4,6-Dimethylpyrimidine.

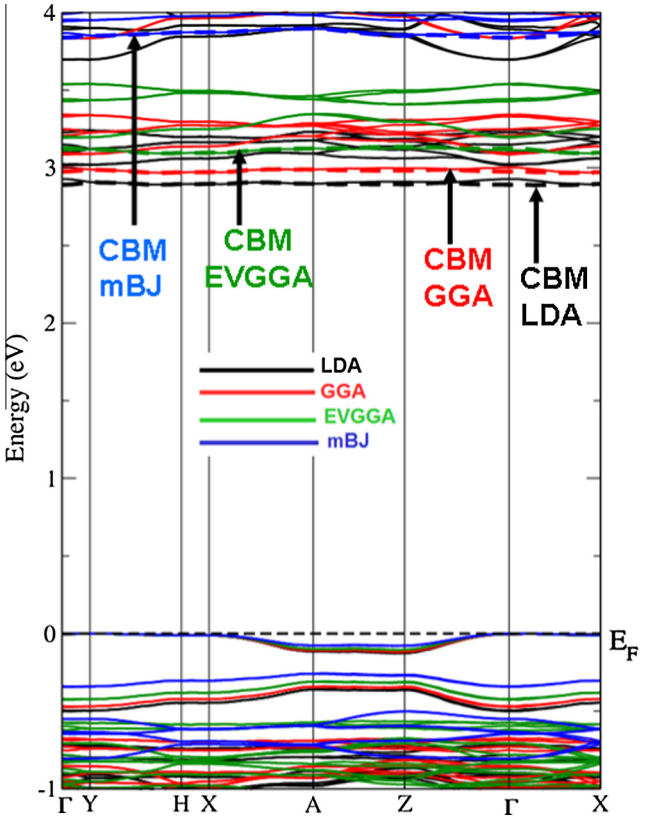

Fig. 2. The calculated electronic band structure of Benzoic Acid 2-Amino-4,6-Dimethylpyrimidine using four exchange correlation potentials LDA, GGA, EVGGA and mBJ.

Acid 2-Amino-4,6-Dimethylpyrimidine is a direct band gap semiconductor in good agreement with the previously calculated electronic band structure using CASTEP code within *PBE-GGA* [1]. The calculated band gap is about 2.888 eV (*LDA*), 2.965 eV (*PBE-GGA*), 3.090 eV (*EV-GGA*) and 3.838 eV (*mBJ*). We would like to mention that Li et al. [1] have calculated the energy band gap of Benzoic Acid 2-Amino-4,6-Dimethylpyrimidine to be 3.0271 eV using CASTEP code within *PBE-GGA*. It is well known that *PBE-GGA* underestimate the energy band gap by around 10–30% [14,15]. To overcome this drawback we proposed *mBJ*. The *mBJ*, a modified Becke–Johnson potential, allows the calculation of band gaps with accuracy similar to the very expensive *GW* calculations [13]. It is a local approximation to an atomic "exact-exchange" potential and a screening term. Since the exact value of the experimental band gap is not reported in the literature, therefore based on our previous calculation [6,7,16] of the band gap using *mBJ* for several systems whose energy band gap are known experimentally, in those previous calculations we found very good agreement with the experimental data. Thus, we believe that our calculations reported in this paper would produce very accurate and reliable value of the energy band gap.

The calculated total density of states (*TDOS*) as illustrated in Fig. 3(a) confirms there is significant influence on the band/state dispersion when one move from *LDA* → *PBE-GGA* → *EV-GGA* → *mBJ*. The *TDOS* support the previous finding from the electronic band structure that the *CBM* shift toward higher energies resulting in increasing the band gap's value, and *mBJ* cause to increase the band gap's value by around 1.0 eV over the value obtained from *LDA*. Therefore, we choose *mBJ* to calculate the partial density of states (*PDOS*). The C-s/p, H-s, N-s/p and O-s/p partial density of states are represented in Fig. 3(b) and (c). From the *PDOS* we can identify the angular momentum characters of various structures. There exists a strong hybridizations between C-s/p, H-s, N-s/p and O-s/p states above and below the Fermi level (E_F). Which may led to covalent bonding between the states. It is clear that the C-s/p, H-s, N-s/p and O-s/p states contribute along the whole energy range. The *VBM* is mainly formed by N-p state while the *CBM* is formed by the strongly hybridized N-p and C-p states.

The partial density of states below E_F (*VB-PDOS*) in the energy range between -9.0 and 0.0 eV, show that the O-p state is the dominant (1.5 electron/eV) among the other states. The next is C-p state with contribution of about (0.6 electron/eV) and N-p (0.55 *electron/eV*). Whereas N-s contribute by around (0.125 electron/eV), O-s and C-s by around (0.08 electron/eV), and finally H-s exhibit the lowest contribution in this region (0.05 electron/eV). This different contribution indicating that there are some electrons from O-s/p, C-s/p, N-s/p and H-s states are transferred into valence bands and contribute in covalence interactions which is due to the strong hybridization between these states.

To provide a deep insight into the electronic structure we have taken a deep careful look at valence band's electronic charge density distribution to visualizes the charge transfer and the chemical bonding characters. The total valence charge density is calculated in two crystallographic planes namely (0 0 1) and (1 0 1) as illustrated in Fig. 4(a) and (b). The crystallographic plane (0 0 1) exhibit only N, C and H atoms. Due to electro-negativity difference between N (3.04) and C (2.55) one can see the charge transfer toward N atoms as indicated by the blue color (according to the thermoscale the blue color exhibit the maximum charge) also one can see the existence of the covalent bond between N and C atoms. In addition we have plotted the (1 0 1) crystallographic plane, in which all atoms are contribute. This plane show the covalent bonds between C–C, C–N and C–O atoms, the charge transfer toward O and N atoms and the maximum charge accumulated around them. Also it shows that the 2-Amino-4,6-Dimethylpyrimidine molecule linked to benzoic acid molecule by two hydrogen bonds [$O1-H1\cdots N1, H\cdots N = 1.815$ Å; $N3-H3A\cdots O2, H\cdots O = 2.149$ Å] to form the asymmetric unit. The calculated bond distance show good agreement with previously measured one (1.819 Å and 2.157 Å) [1]. The molecules of the asymmetric unit are connected in dimers by $N-H\cdots O$ and $O-H\cdots N$ hydrogen bonds. The calculated bond distances, angles and torsion angles along with the experimental data [1] are listed in Tables S2, S3 and S4 (supplementary materials), good agreement was found.

3.2. Linear optical properties

The optical properties helps to get deep insight into the electronic structure, therefore we have calculated the optical properties of Benzoic Acid 2-Amino-4,6-Dimethylpyrimidine within the recently modified Becke–Johnson potential (*mBJ*). Since *mBJ* is expected to bring the calculated energy band gap close to the experimental one, therefore we expected the electric-dipole transitions occurs between the exact valence and the conduction bands to allow the valid optical transition. It is well known that the exact form of exchange-correlation functional is unknown. Therefore the accuracy of our results will be sensitive to selection of the exchange-correlation functional and it can play a major role for the accuracy of the results and this is one of the main drawback in DFT. Benzoic Acid 2-Amino-4,6-Dimethylpyrimidine possess five non-zero components of the second-order optical dielectric tensor corresponding to the electric field $\vec{E}$ being directed along **a**, **b**, and **c**-crystallographic axes. These are $\varepsilon^{xx}(\omega)$, $\varepsilon^{xy}(\omega)$, $\varepsilon^{xx}(\omega)$, $\varepsilon^{yx}(\omega)$ and $\varepsilon^{zz}(\omega)$, here we will concentrate only on the dominate components correspond to the transitions that have large optical matrix elements i.e. $\varepsilon^{xx}(\omega)$, $\varepsilon^{yy}(\omega)$ and $\varepsilon^{zz}(\omega)$corresponding to [1 0 0], [0 1 0] and [0 0 1] polarization directions. Therefore, the imaginary part

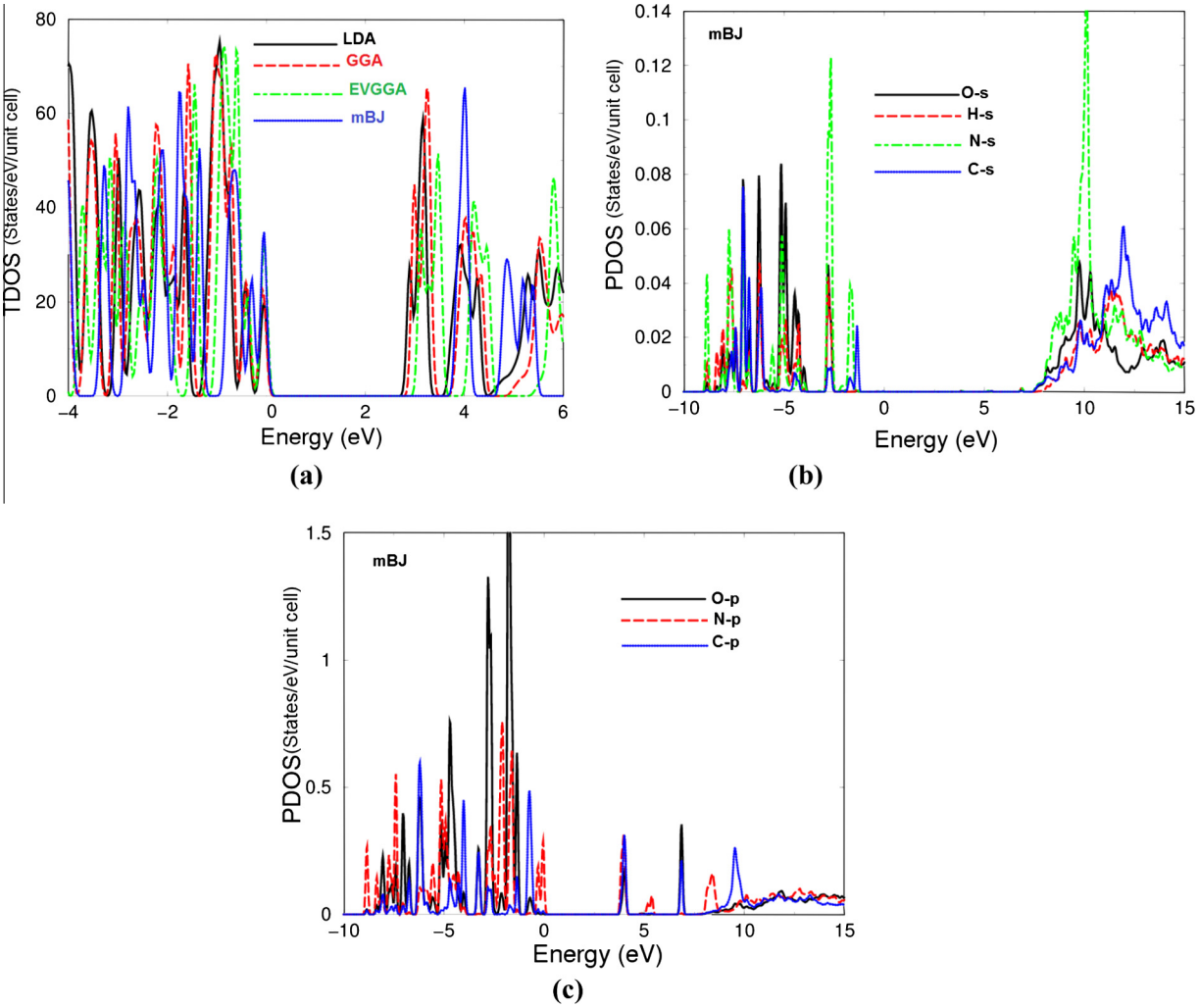

Fig. 3. (a) Calculated total density of states (states/eV/unit cell) using LDA, GGA, EVGGA and mBJ; (b) calculated partial density of states (states/eV/unit cell) using mBJ.

$\varepsilon_2^{xx}(\omega)$, $\varepsilon_2^{yy}(\omega)$ and $\varepsilon_2^{zz}(\omega)$ of the optical function's dispersion are completely defines the linear optical properties. These are originates from inter-band transitions between valence and conduction bands. Broadening is taken to be 0.1 eV which is typical of the experimental accuracy.

The expression for calculating the imaginary part are given elsewhere [17]. Fig. 5(a) exhibits the imaginary part of the optical function's dispersion, it is clear that the first transition occurs at 3.838 eV. The first spectral transition occurs between C-s and N-s states in the valence band to N-p, C-p and O-p states of the conduction band. The main spectral structure is situated at 5.5 eV which is dominated by the optical component corresponding to [001] polarization directions. The main spectral structure is due to the optical transitions between H-s, O-s/p, C-s/p and N-s/p states of the VBs to O-p, N-p and C-p states of the CBs. It is clear that both of $\varepsilon_2^{xx}(\omega)$ and $\varepsilon_2^{zz}(\omega)$ exhibit pronounced structure in comparison to $\varepsilon_2^{yy}(\omega)$ and they show considerable anisotropy with $\varepsilon_2^{zz}(\omega)$. Thus, the Benzoic Acid 2-Amino-4,6-Dimethylpyrimidine is uniaxial crystal. The spectral structure exhibit that there exists four lossless regions situated at 5.0, 6.7, 7.9 and 8.9 eV.

We can derive the real parts $\varepsilon_1^{xx}(\omega)$, $\varepsilon_1^{yy}(\omega)$ and $\varepsilon_1^{zz}(\omega)$ of the optical function's dispersion from the imaginary parts using the Kramers–Kronig transformation [18]. These are represented in Fig. 5 (b). Again it shows there exists a considerable anisotropy between both of $\varepsilon_1^{xx}(\omega)$ and $\varepsilon_1^{zz}(\omega)$ with $\varepsilon_1^{yy}(\omega)$ confirming that the investigated crystal is a uniaxial crystal. The uniaxial anisotropy $\delta\varepsilon = [(\varepsilon_0^{\parallel} - \varepsilon_0^{\perp})/\varepsilon_0^{tot}]$ is found to be 0.2, indicating the existence of the considerable anisotropy. The calculated values of $\varepsilon_1^{xx}(0)$, $\varepsilon_1^{yy}(0)$ and $\varepsilon_1^{zz}(0)$ obtained by *LDA*, *GGA* and *EVGGA* and *mBJ* are listed in Table 1. These values could explain the influence of the exchange correlation potential on the energy gap's value and hence on the optical properties. We noticed that *mBJ* gives the lowest values. Thus, the larger $\varepsilon_1(0)$ value is corresponding to the small energy gap. This could be explained on the basis of the Penn model [19]. Penn proposed a relation between $\varepsilon(0)$ and E_g, $\varepsilon(0) \approx 1 + (\hbar\omega_P/E_g)^2$. E_g is some kind of averaged energy gap which could be related to the real energy gap. It is clear that $\varepsilon(0)$ is inversely proportional with E_g. Hence a larger E_g yields a smaller $\varepsilon(0)$. This finding support our previous observation from the calculated electronic band structure and the density of states which shows that *LDA*, *PBE-GGA* and *EV-GGA* are underestimated the energy band gap, while *mBJ* success by large amount to bring the calculated energy band gap closer to the experimental one.

We can derive the reflectivity spectra $R(\omega)$, absorption coefficient $I(\omega)$, the electron loss function $L(\omega)$ and the optical conductivity $\sigma(\omega)$ from the imaginary and real parts of the optical function's dispersion.

The optical reflectivity as a function of photon energy is illustrated in Fig. 5(c). At low energy region the investigated crystal exhibit low reflectivity of about 0.035 for $R^{xx}(\omega)$, 0.01 for $R^{yy}(\omega)$

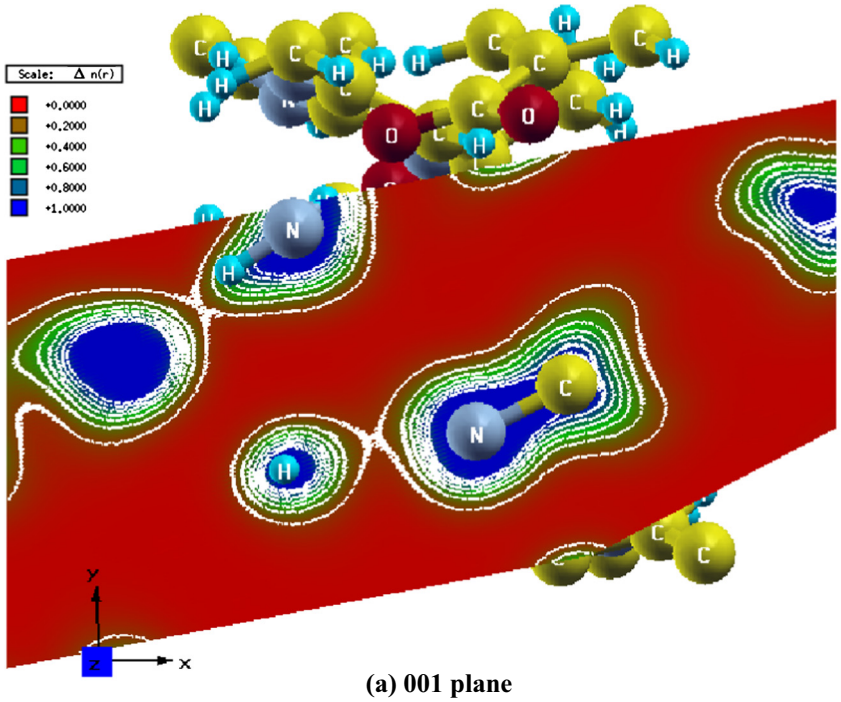

(a) 001 plane

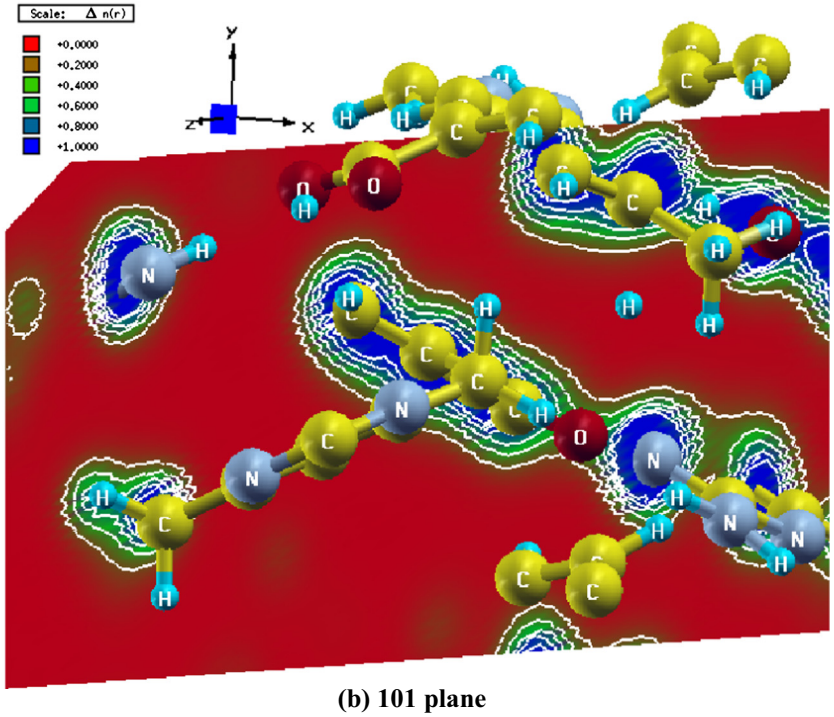

(b) 101 plane

Fig. 4. The electron charge density distribution were calculated for; (a) (0 0 1) crystallographic plane and (b) (1 0 1) crystallographic plane.

and 0.04 for $R^{zz}(\omega)$, then a rapid increases in the spectra to form the first reflectivity maxima (25%) at around 4.5 eV. The main reflectivity maxima (65%) occurs at around 6.38 eV (~194 nm) which is longer from the optical absorption wavelength but better than that obtained by Li et al. (6.59 eV, ~188 nm) [1]. The main reflectivity maxima is followed by the first reflectivity minima (6.7 eV). The second and third reflectivity minimum occurs at around 7.9 and 8.9 eV. The reflectivity minimum confirm the occurrence of a collective plasmon resonance. The depth of the plasmon minimum is determined by the imaginary part of the frequency dependent optical dielectric function at the plasma resonance and is representative of the degree of overlap between the inter-band absorption regions.

Fig. 5(d) represents the absorption coefficient $I(\omega)$ of the investigated crystal, it show there are four absorption bands separated by lossless regions. The first one is low absorption region while the second one is the highest absorption region in which the crystal exhibit high transparency. This strong absorption peak appear at around 5.5 eV (~226 nm) which is comparable with the experimental value 229 nm [1] and much better than that obtained by

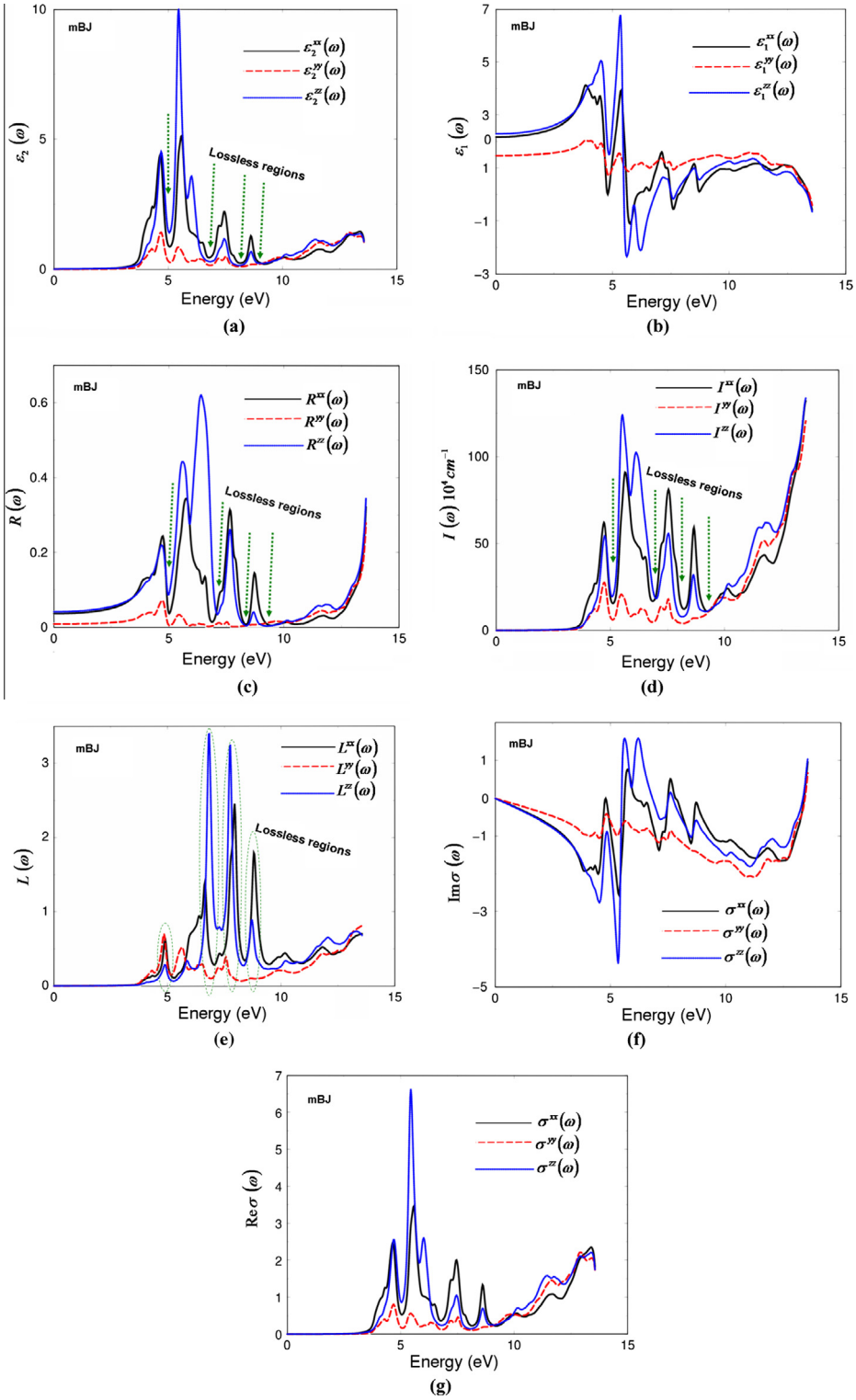

Fig. 5. (a). Calculated $\varepsilon_2^{xx}(\omega)$ (dark solid curve–black color online), $\varepsilon_2^{yy}(\omega)$ (light dashed curve–red color online) and $\varepsilon_2^{zz}(\omega)$ (light dotted curve–blue color online) spectra. (b). Calculated $\varepsilon_1^{xx}(\omega)$ (dark solid curve–black color online), $\varepsilon_1^{yy}(\omega)$ (light dashed curve–red color online) and $\varepsilon_1^{zz}(\omega)$ (light dotted curve–blue color online) spectra. (c). Calculated $R^{xx}(\omega)$ (dark solid curve–black color online), $R^{yy}(\omega)$ (light dashed curve–red color online) and $R^{zz}(\omega)$ (light dotted curve–blue color online) spectra. (d) Calculated $I^{xx}(\omega)$ (dark solid curve–black color online), $I^{yy}(\omega)$ (light dashed curve–red color online) and $I^{zz}(\omega)$ (light dotted curve–blue color online) spectra. The absorption coefficient in 10^4 s^{-1}. (e) Calculated $L^{xx}(\omega)$ (dark solid curve–black color online), $L^{yy}(\omega)$ (light dashed curve–red color online) and $L^{zz}(\omega)$ (light dotted curve–curve–blue color online) spectra. (f) Calculated $Im\sigma^{xx}(\omega)$ (dark solid curve–black color online), $Im\sigma^{yy}(\omega)$ (light dashed curve–red color online) and $Im\sigma^{zz}(\omega)$ (light dotted curve–blue color online) spectra. (g) Calculated $Re\sigma^{xx}(\omega)$ (dark solid curve–black color online), $Re\sigma^{yy}(\omega)$ (light dashed curve–red color online) and $Re\sigma^{zz}(\omega)$ (light dotted curve–blue color online) spectra. (For interpretation of the references to color in this figure legend, the reader is referred to the web version of this article.)

CASTEP code with *PBE-GGA* (5.68 eV, ~218 nm) [1]. The strong absorption peak is corresponding to $\pi \rightarrow \pi^*$ transitions [1,20–23]. To clearly show the lossless regions we plot the loss function $L(\omega)$ as shown in Fig. 5(e) which confirm the existence of the lossless regions at 5.0, 6.7, 7.9 and 8.9 eV in coincidence with our observation in Fig. 5(a–d). The loss function's peaks represent the

Table 1
Calculated $\varepsilon_1^{xx}(0)$, $\varepsilon_1^{yy}(0)$ and $\varepsilon_1^{zz}(0)$.

	LDA	GGA	EV-GGA	mBJ
$\varepsilon_1^{xx}(0)$	3.06	2.94	2.76	2.16
$\varepsilon_1^{yy}(0)$	2.16	2.04	1.84	1.47
$\varepsilon_1^{zz}(0)$	3.22	3.05	2.87	2.28

plasma frequencies (ω_P). We should emphasize that above ω_P the material behaves as dielectric where $\varepsilon_1(\omega)$ is positive, while below ω_P where $\varepsilon_1(\omega)$ is negative the material exhibit metallic nature. The loss function $L(\omega)$ is represented in Fig. 5(d).

In Fig. 5(f) and (g) we have represented the calculated imaginary and real parts of the optical conductivity dispersion $\mathrm{Im}\,\sigma(\omega)$ and $\mathrm{Re}\,\sigma(\omega)$. Again it shows the existence of the considerable anisotropy among $\sigma^{xx}(\omega)$ and $\sigma^{zz}(\omega)$, and the real part confirm the existence of the lossless region at 5.0, 6.7, 7.9 and 8.9 eV in coincidence with our previous observation. The optical conductivity is related to the frequency-dependent dielectric function $\varepsilon(\omega)$ as $\varepsilon(\omega) = 1 + \frac{4\pi i\sigma(\omega)}{\omega}$. The peaks in the optical conductivity spectra are determined by the electric-dipole transitions between the occupied states and the unoccupied states.

4. Conclusions

We have used the X-ray diffraction data of Benzoic Acid 2-Amino-4,6-Dimethylpyrimidine (1:1) co-crystal for comprehensive theoretical calculation using the density function theory within different kinds of exchange and correlation potentials. The atomic positions were optimized by minimization of the forces acting on each atom. From the relaxed geometry we have calculated the electronic band structure, total and partial density of states, electronic charge density distribution and the optical properties. The calculated partial density of states helps to identify the angular momentum character of the various structures and the hybridizations between the states to identify the bonding nature. The electronic band structure exhibit that the Benzoic Acid 2-Amino-4, 6-Dimethylpyrimidine is a direct band gap semiconductor. The calculated band gap is about 2.888 eV (*LDA*), 2.965 eV (*PBE-GGA*), 3.090 eV (*EV-GGA*) and 3.838 eV (*mBJ*) in comparison with the previously calculated band gap 3.0271 eV using CASTEP code within *PBE-GGA*. From the partial density of states we found that the valence band maximum is originated from N-p state while the conduction band minimum is formed by the strongly hybridized N-p and C-p states. There exists a strong hybridizations between C-s/p, H-s, N-s/p and O-s/p states above and below the Fermi level (E_F). Which may led to covalent bonding between the states. To visualizes the charge transfer and the chemical bonding characters, the valence band's electronic charge density distribution were extensively investigated. The optical properties helps to get deep insight into the electronic structure therefore, details analysis to the calculated optical properties were performed. The optical properties confirm the existence of the band gap and the lossless regions.

Acknowledgments

The result was developed within the CENTEM project, reg. no. CZ.1.05/2.1.00/03.0088, cofunded by the ERDF as part of the Ministry of Education, Youth and Sports OP RDI programme and, in the follow-up sustainability stage, supported through CENTEM PLUS (LO1402) by financial means from the Ministry of Education, Youth and Sports under the "National Sustainability Programme I. Computational resources were provided by MetaCentrum (LM2010005) and CERIT-SC (CZ.1.05/3.2.00/08.0144) infrastructures.

Appendix A. Supplementary material

Supplementary data associated with this article can be found, in the online version, at http://dx.doi.org/10.1016/j.optmat.2015.04.022.

References

[1] Z. Li, J. Huang, A. Meng, B. Zheng, Crystal structure, energy band and optical properties of benzoic acid-2-amino-4,6-dimethylpyrimidine (1:1) co-crystals, J. Struct. Chem. 51 (2010) 53–59.
[2] S.P. Goswami, K. Ghosh, Molecular recognition: chain length selectivity studies of dicarboxylic acids by the cavity of new Troger's base receptors, Tetrahedron Lett. 38 (1997) 4503–4506.
[3] S.P. Goswami, A.K. Mahapatra, G.D. Nigam, K. Chinnakali, H.K. Fun, N-(3-Hydroxyphenyl-)-p-toluenesulfonarnide, Acta Crystallogr. A C54 (1998) 1301–1302.
[4] Z. Latajka, G. Gajewski, A.J. Barnes, H. Ratajczak, Hyperpolarizabilities of strongly hydrogen-bonded molecular complexes: PM3 and ab initio studies, J. Mol. Struct. 844–845 (2007) 340–342.
[5] A.H. Reshak, X. Chen, S. Auluck, H. Kamarudin, Linear optical susceptibilities of the oxoborate $(Pb_3O)_2(BO_3)_2WO_4$: theory and experiment, J. Mater. Sci. 47 (2012) 5794–5800.
[6] A.H. Reshak, H. Kamarudin, S. Auluck, Dispersion of the linear and nonlinear optical susceptibilities of disilver germanium sulfide from DFT calculations, J. Mater. Sci. 48 (2013) 1955–1965.
[7] A.H. Reshak, I.V. Kityk, O.V. Parasyuk, A.O. Fedorchuk, Z.A. Alahmed, N. AlZayed, H. Kamarudin, S. Auluck, X-ray photoelectron spectrum, X-ray diffraction data, and electronic structure of chalcogenide quaternary sulfide $Ag_2In_2GeS_6$: experiment and theory, J. Mater. Sci. 48 (2013) 1342–1350.
[8] B. Merabet, Y. Al-Douri, H. Abid, A.H. Reshak, Electronic and optical properties of $(Al_xGa_{12x})_{12y}Mn_yAs$ single crystal: a new candidate for integrated optical isolators and spintronics, J. Mater. Sci. 48 (2013) 758–764.
[9] P. Blaha, K. Schwarz, G.K.H. Madsen, D. Kvasnicka, J. Luitz, WIEN2k, An Augmented Plane Wave Plus Local Orbitals Program for Calculating Crystal Properties, Vienna University of Technology, Austria, 2001.
[10] W. Kohn, L.J. Sham, Self-consistent equations including exchange and correlation effects, Phys. Rev. A 140 (1965) 1133.
[11] J.P. Perdew, S. Burke, M. Ernzerhof, Generalized gradient approximation made simple, Phys. Rev. Lett. 77 (1996) 3865.
[12] E. Engel, S.H. Vosko, Exact exchange-only potentials and the virial relation as microscopic criteria for generalized gradient approximations, Phys. Rev. B 47 (1993) 13164.
[13] F. Tran, P. Blaha, Accurate band gaps of semiconductors and insulators with a semilocal exchange-correlation potential, Phys. Rev. Lett. 102 (2009) 226401.
[14] Y. Zhao, D.G. Truhlar, Calculation of semiconductor band gaps with the M06-L density functional, J. Chem. Phys. 130 (2009) 074103.
[15] H. Xiao, J. Tahir-Kheli, W.A. Goddard, Accurate band gaps for semiconductors from density functional theory, J. Phys. Chem. Lett. 2 (2011) 212–217.
[16] A.H. Reshak, I.V. Kityk, O.V. Parasyuk, H. Kamarudin, S. Auluck, Influence of replacing Si by Ge in the chalcogenide quaternary sulfides $Ag_2In_2Si(Ge)S_6$ on the chemical bonding, linear and nonlinear optical susceptibilities, and hyperpolarizability, J. Phys. Chem. B 117 (2013) 2545–2553.
[17] F. Bassani, G.P. Parravicini, Electronic States and Optical Transitions in Solids, Pergamon Press Ltd., Oxford, 1975. pp. 149–154.
[18] F. Wooten, Optical Properties of Solids, Academic press, New York and London, 1972.
[19] D.R. Penn, Wave-number-dependent dielectric function of semiconductors, Phys. Rev. B 128 (1962) 2093.
[20] M. Florio Gina, S. Zwier Timothy, M. Myshakin Evgeniy, D. Jordan Kenneth, L. Sibert Edwin, Theoretical modeling of the OH stretch infrared spectrum of carboxylic acid dimers based on first-principles anharmonic couplings, J. Chem. Phys. 118 (2003) 1735.
[21] J.R. Zamian, E.R. Dockal, Tetradentate Schiff base oxovanadium(IV) complexes, Transition Met. Chem. 21 (1996) 370.
[22] O. Signorini, E.R. Dockal, G. Castellano, G. Oliva, Synthesis and characterization of aquo[N,N′-ethylenebis(3-ethoxysalicylideneaminato)]dioxouranium(VI), Polyhedron 15 (1996) 245–255.
[23] S. Zolezzi, A. Decinti, E. Spodine, Syntheses and characterization of copper(II) complexes with Schiff-base ligands derived from ethylenediamine, diphenylethylenediamine and nitro, bromo and methoxy salicylaldehyde, Polyhedron 18 (1999) 897–904.